Impact of extreme electrical fields on charge density distributions in Al_3Sc alloy

Claudia Loyola and Joaquin PeraltaScott R. Broderick and Krishna Rajan

Citation: Journal of Vacuum Science & Technology A: Vacuum, Surfaces, and Films **34**, 061404 (2016); doi: 10.1116/1.4964833

View online: http://dx.doi.org/10.1116/1.4964833

View Table of Contents: http://avs.scitation.org/toc/jva/34/6

Published by the American Vacuum Society

Impact of extreme electrical fields on charge density distributions in Al_3Sc alloy

Claudia Loyola[a] and Joaquin Peralta
Facultad de Ciencias Exactas, Departamento de Ciencias Físicas, Universidad Andrés Bello, Sazié 2212, Santiago 8370136, Chile

Scott R. Broderick and Krishna Rajan
Department of Materials Design and Innovation, University at Buffalo, The State University of New York, 126 Bell Hall, Buffalo, New York 14260-5030

(Received 19 May 2016; accepted 3 October 2016; published 14 October 2016)

In this study, the authors investigated how extreme electrical fields affect charge distribution of metallic surfaces and bond character at the moment of evaporation. The surface structure and neighborhood chemistry were also studied as a function of various field evaporation pathways. Density functional theory (DFT) was used to model the surface bonding and charge distribution and then correlate the DFT results with experimental results by comparing the calculated evaporation fields with atom probe tomography measurements. The evaporation fields of different surface neighborhood chemistries in $L1_2$-Al_3Sc were calculated, with the Sc atoms occupying the corners of a cubic unit cell and the Al atoms occupying the face centers. Al-Al surface atoms are found via DFT to be more likely to evaporate as dimers because of the Al-Al shared charge density. In contrast, Al-Sc evaporates as single ions due to the increased density localized around the Sc atom. This difference in evaporation behavior correlates with the resistance to degradation under extreme fields. This work allows better interpretation of the atom probe data by clarifying the relationship between different evaporation events and the role of surface and subsurface chemistry. [http://dx.doi.org/10.1116/1.4964833]

I. INTRODUCTION

Atom probe tomography (APT) is a characterization method that provides reconstructed 3D spatial coordinates and chemistry of each detected atom with subnanometer and parts per million resolutions, respectively.[1–4] This method operates based on the physics of field evaporation, so fully understanding the governing physics is beneficial for properly interpreting the APT outputs. The concept of theory-based modeling of the field evaporation process has been ongoing for nearly half a century,[2,3] and recently, the modeling has been expanded to further consider the APT evaporation process.[5–13] In this paper, we build on these prior works to define the critical bonding character (i.e., change in charge distribution) that leads to field evaporation for specific chemical distributions. This fundamental study on defining this critical character as a function of surface chemistry, and particularly the distribution between *specific* chemical neighborhoods, provides a model of chemistry-charge distribution relationships that directly lead to field evaporation.

The theoretical basis builds on the work of Forbes *et al.*,[14–19] who modeled the evaporation field for specific atoms on a curved surface by mathematically accounting for the bonding energy, thermodynamics of surface diffusion, and defined curvature-dependent corrections. This approach is foundational for understanding APT results, which takes into account the field evaporation of curved surfaces. The theory is built on the Fowler–Nordheim formula, which quantitatively describes field emission in metals, and which was later modified through a semiclassical approximation.[20,21] Of interest for us is that this work was able to define the surface behavior of specific metallic atoms under electric field, as opposed to capturing only the general chemical behavior. Building on these described physics principles, Kreuzer modeled evaporation behavior of different ion charge states, multi-ion evaporations, and the distribution of charge throughout the entire material via density functional theory (DFT).[21–23] More recent works have explored the structural changes, charge transfer, and desorption pathways of nonconducting materials during field evaporation.[24–27] These calculations described the change in potential energy as a function of applied field, from which the evaporation fields of the atoms were extracted. From these calculations, the distortion of the electronic orbitals and the weakening/strengthening of the local molecular bonding orbital are described. Interestingly, in nonmetals, the electric field is distributed across the sample, while in metals only the surface layer is affected due to field expulsion.[26] Thus, a cluster of a few layers is sufficient for modeling the field evaporation of conducting materials.

In another recent DFT study on field evaporation of metal surfaces, Yao *et al.* defined the differences in evaporation field as a function of shape, and particularly focused on atoms that deviated from the spherical surface.[28] The study also addressed evaporation sequence and corresponding depth and spatial resolution. The DFT results were in agreement with the experimental APT evaporation maps, and, overall, this work provided an improved understanding of the aberrations associated with nonideal surface features. In

[a]Electronic mail: claudia.loyola@unab.cl

the paper's conclusion, Yao *et al.* proposed that a future challenge would be to simulate the evaporation behavior of a material in which each atom's evaporation field is dependent on its neighbors' chemistries. This is the challenge that we address in the present paper.

Further, we build on our prior work of linking experimental measurements with theory to quantitatively report the difference in evaporation field between single- and multiple-ion evaporations.[29] While the calculations in that work were not as theoretically rigorous as the calculations of Forbes,[14–19] we demonstrated that these were qualitatively accurate based on the relationships experimentally measured using APT. Our contribution here extends our previous studies to describe the bonding character represented through the charge density distributions for specific chemical neighborhoods. Our current data also show differences in evaporation fields with consideration given for both single ion and dimer evaporations. Through this theory-driven study of change in surface charge density as a function of electric field, we correlate the bonding properties and surface degradation under extreme environments. This work provides the basis for understanding the electronic charge distribution at the moment of field evaporation in metallic surfaces, as a function of the number of ions evaporated, structure, and surface chemistry.

II. BACKGROUND

A. Computational details

The field evaporation process was computationally characterized by modeling the charge density at the surface of the material as a function of electric field, thereby identifying the charge distribution and directionality just prior to field evaporation. In addition, the electron localization function (ELF) was analyzed just prior to evaporation. Like in our prior work,[29] calculations were performed using QUANTUM-ESPRESSO (QE)[30] for DFT with generalized gradient approximation. The QE-software supports multiple methods to incorporate an electric field. We used a sawlike potential because it works best for surfaces, but there also are other methods to consider semimetallic and ceramic surfaces. The Al_3Sc cell contained 80 atoms with (111) orientation along the z-axis. A single ion or dimer are placed at the surface, with four different configurations modeled (Al, Sc, Al-Al, and Al-Sc at the surface). The energy cutoff used was 200 Rydberg and the Marzari-Vanderbilt scheme was employed.[31] A dipole correction was used to incorporate the electric field.[32] The values identified for evaporation fields for Al, Sc, Al-Al, and Al-Sc from our prior work are 29, 32, 25, and 36 V/nm, respectively. Minimized energy structures with and without the presence of an electric field have been relaxed using the quasi-Newton technique, with a $2 \times 2 \times 2$ K-point mesh grid. The initial surface and the evaporation process we are modeling are shown in Fig. 1, for the case of Al-Sc dimer evaporation.

The electronic charge density and the ELF (Refs. 33 and 34) were calculated in order to characterize the bond-breaking process between the evaporating ions and the Al_3Sc surface when a high electric field is present. In order to isolate the role of electric field, bonding conditions with no field also were modeled. The electric field values used here correspond to just below the evaporation field (F_e) values previously calculated because the main electron densities will be present just prior to evaporation. The electric fields used for Al-Al and Al-Sc ad-atoms were 22 and 33 V/nm, respectively. A higher grid of K-point mesh ($6 \times 6 \times 4$) has been used in the self-consistent calculation to improve the electronic results.

To determine the charge density of the bond between the dimer and the surface, three different charge densities have been calculated. The first is an initial charge density ρ_0 that corresponds to the charge density of the full system, the second is the charge density associated with the surface without the dimer ρ_1, and the third is the charge density of only the dimer ρ_2. The final charge density of the bond was determined using

$$\rho_{\text{bond}} = \rho_0 - \rho_1 - \rho_2. \quad (1)$$

The ELF is a mathematical function that is used to determine the properties of the bonding in a crystal between the different atomic species. The function values are defined between 0 and 1, with the value giving us information about the nature of the atomic bond. For example, an ELF-value between 0.3 and 0.6 is mainly a metallic bond, and higher values (~0.8 or higher) are characteristic of a covalent bond. Therefore, by utilizing ELF in this work, we define charge density at the bond just prior to evaporation and also the nature of the bonding.

B. Experimental details

The APT results shown in this paper are for an Al-3.65 Mg-0.06Sc (at. %) alloy. For APT, a LEAP 3000× was used in voltage mode, with a flight length of 160 mm, a fixed temperature of approximately 35 K, and pressure of 7.5×10^{-9} Pa. A

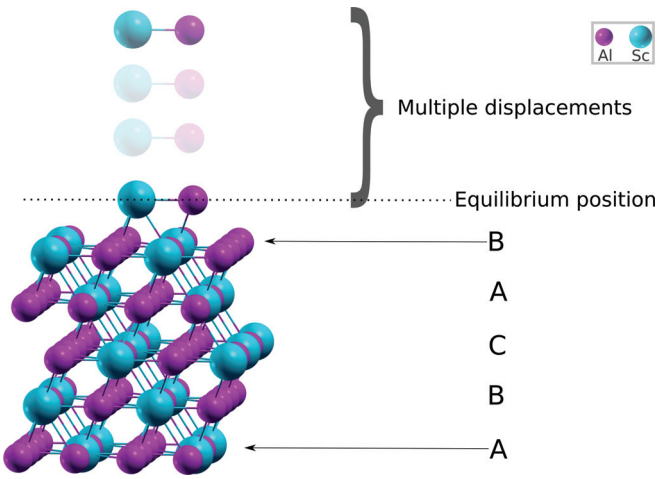

FIG. 1. (Color) Initial slab of Al_3Sc with A-B-C layer scheme for the surface. The evaporated ion or dimer is placed at the surface and an electric field is applied. The charge density that contributes to the evaporation of the surface ion(s), here an Al-Sc dimer, is modeled in this figure. That is, correlation between surface bonding and behavior under extreme environments is assessed here.

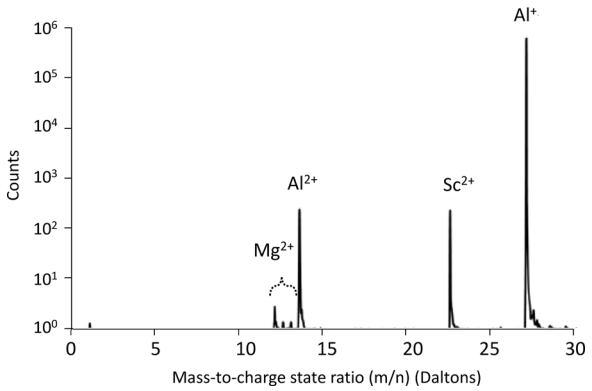

FIG. 2. Mass-to-charge spectra of the Al-Sc precipitates from APT. These experimental measures of the $L1_2$ precipitate provide a comparison with the $L1_2$-Al_3Sc DFT calculations.

pulse fraction of 0.10–0.15 and average evaporation rate of 5 $\times$ 10^{-3} ion per pulse were used. The percentage of detected multihits compared to the overall hits was 17%. The primary region of interest for this paper is the $L1_2$ Al-Sc precipitates. In this sample, the number of Al^{2+} and Sc^{2+} ions collected was nearly equivalent, as is shown in the mass-to-charge spectra for the precipitates (Fig. 2). This nearly equivalent amount of Al^{2+} and Sc^{2+} ions was the result of the analysis and was not due to any specific selection of experimental or reconstruction parameters. Other peaks corresponding with molecular ions appeared only in small quantities and are not considered in this analysis. Other analyses of this material for different objectives are provided in the literature.[35–37]

III. CHARGE DENSITY RESULTS

The effects of electric field on the single Al and Sc adatoms are presented in Fig. 3. We observed a significant modification in charge distribution surrounding the ion when the evaporation field was incorporated. In the figure, red

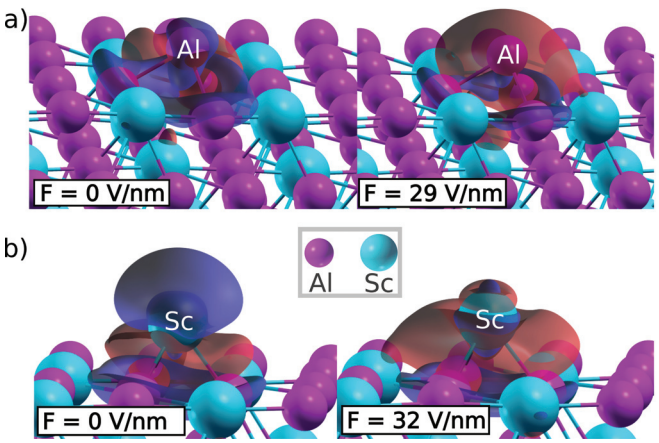

FIG. 3. (Color) Charge densities for Al (a) and Sc (b) atoms on Al_3Sc surface with no electric field (left) and under electric field (right) (29 and 32 V/nm for Al and Sc, respectively). The colors represent the charge densities of $+0.0015$ e/bohr^3 (red) and -0.0015 e/bohr^3 (blue). The differences between the samples provide an insight into the different evaporation mechanisms of Al and Sc under electric field.

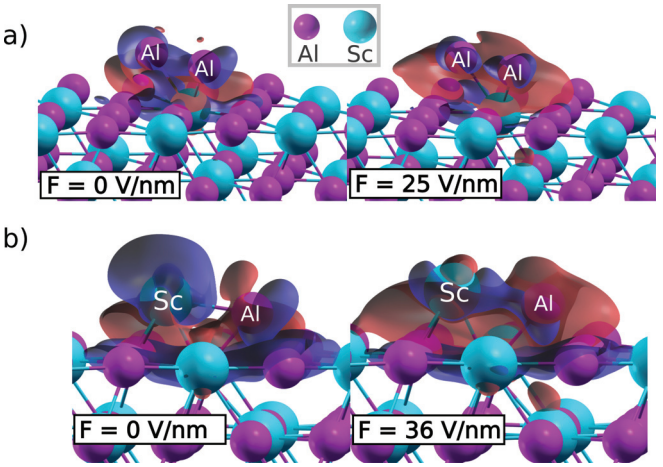

FIG. 4. (Color) Charges densities for Al-Al (a) and Al-Sc (b) dimers with no electric field (left) and with electric field applied (right).

indicates a positive charge per volume and blue a negative charge per volume. The values of $\pm 1.5 \times 10^{-3}$ e/bohr^3 were chosen as the main representative values for observing changes in the bonding.

The results of the charge density calculations in the sample (surface plus adatoms), under no electric field and with electric field just below the evaporation field, are shown for the Al-Al dimer and Al-Sc dimer in Fig. 4. This figure presents the difference in charge density for the bonds of interest, allowing us to define the planes of interest. For the Al-Al dimer, shown in Fig. 4(a), we observe two principal planes of interest for the charge density. The first, P_1AlAl, corresponds to the plane that crosses the dimer atoms and one Sc atom from the surface (Sc_s) with which the dimer atoms are bonded. We find that they share charge density. The second plane, P_2AlAl, is defined by one Al atom of the dimer and two atoms from the surface, Sc_s and Al_s. The bond between these atoms corresponds to a significant charge density.

For the Al-Sc dimer on the surface, shown in Fig. 4(b), we can observe three principal planes of interest associated with the charge density between the dimer and the surface. The first plane, P_1AlSc, is defined for the dimer atoms and one aluminum atom from the surface (Al_1). The second plane, P_2AlSc, is defined by the Al atom of the dimer and two Al atoms from the surface: Al_1 and one $Al(Al_2)$ atom that is close to the dimer and has a shared charge density with the other atoms. The last plane, P_3AlSc, corresponds to the Sc atom of the dimer and two surface atoms: Al_1 and $Al(Al_3)$ atom that is close to the Sc atom of the dimer. These planes of interest were extracted from the charge density and used to calculate the ELF.

Beyond defining the critical bonding changes with increasing electric field, we also identify the difference in evaporation mechanisms. For the Al-Al dimer on the surface, the primary charge is between the surface and the dimer, with the distribution shared between the two Al atoms. This shared charge explains why Al-Al evaporates more easily as a dimer than as single ions. Conversely, the Al-Sc dimer on the surface has a significant charge in between the Al and Sc atoms,

and also isolated charges between the atoms and the surface. This configuration of the charge density describes the mechanism for the atoms evaporating as separate ions. Therefore, by calculating the charge density, we have been able to differentiate two separate evaporation mechanisms based on changing electric field.

IV. CORRELATING CHARGE DENSITY WITH APT EVAPORATIONS

In the previous work of Peralta *et al.*,[27] DFT calculations for field evaporation were correlated with APT data by utilizing ion evaporation maps.[38] In the case of multihit events (that is, more than one ion detected at the same time), the ion evaporation map can be used to plot pairwise interactions. The axes of an ion evaporation map are mass-to-charge (m/n) 1 and m/n 2, where each axis represents one of the ions in a multihit event. The inverted ion order is also included, so that the m/n 1 = m/n 2 line is a line of symmetry. A majority of the multihit events are not due to dimer evaporations, but we address this noise issue by considering only relative differences in the multi-ion events. The ion evaporation map is then correlated with relative bond strengths under extreme field, with the greater likelihood of dimer evaporations indicating an increased bond strength. That is, it is more favorable to break all the surface bonds than to break the single bond between the dimer ions. This is clearly demonstrated in Fig. 4, where there are observed charge build-ups for the surface bonds in the case of Al-Al, and build-up between the Al and Sc atoms in the Al-Sc case.

To correlate the DFT charge density calculations with the APT experimental data, the ion evaporation map is compared with the DFT results in Fig. 5. A direct comparison between Al-Al dimers and Al-Sc dimers can be made by comparing Al^{2+} (m/n = 13.5)/Al^{+} (m/n = 27.0) with Sc^{2+} (m/n = 22.5)/Al^{+}. The reason is that the number of Al^{2+} hits and Sc^{2+} hits in the experiment were nearly equivalent (see Fig. 2). Therefore, any changes in the dimer concentration for these two points are due to increased number of dimers, and not as a result of increased atomic concentration in the material. This comparison of ions allows us to make a qualitative ranking of evaporations, which we otherwise would be unable to do, given the differences in the overall concentration. From the experimental data, we can only compare likelihood of dimer evaporations for Al-Sc versus Al-Al, without being able to make a comparison between dimer and single-ion evaporations. However, when compared with our DFT results, the obvious differences in charge density associated with Al-Al and Al-Sc dimers can be related to the evaporation fields. Specifically, surface Al-Al atoms are more likely to evaporate as a dimer than Al-Sc surface atoms, which are more likely to evaporate as two separate ions.

The proposed cause of the decreased likelihood of dimer evaporations for Al-Sc is due to the charge localization around the atoms, as opposed to the previously seen charge sharing. This figure therefore correlates the evaporation mechanism with the experimental data, providing a level of physics not provided by the experimental data alone.

From the experimental measurements of Al-Al dimers versus Al-Sc dimers, we recognize a significantly larger number of Al-Al dimers, meaning lower evaporation field for Al-Al dimers than Al-Sc dimers, as compared to single-ion evaporations. The corresponding charge densities just prior to evaporation show very different evaporation mechanisms. While the charge between the Al-Sc dimer and the surface is greater than that for Al-Al, there is also much greater charge localization around the Sc atom than is seen around any of the Al atoms. Thus, we propose that greater shared charge density between the surface dimers leads to increased likelihood of dimer evaporation, while localization of charge around one of the dimer ions increases likelihood of single-ion evaporation.

V. ELECTRONIC LOCALIZED FUNCTIONS

ELF provides a description of the bonding character that is not provided in the APT measurements. From the charge densities, we identified the critical planes in terms of bonding. These planes were then used for performing the ELF calculations for Al-Al and Al-Sc dimers, as shown in Fig. 6. In the case of the Al-Al dimer on the surface, two different planes were used for ELF calculations (P_1AlAl and P_2AlAl). In the P_1AlAl plane, the ELF-values of electrons between the dimer atoms ranged between 0.8 and 1.0. We also noted a narrowing of the bond between the adatoms and the Sc atom on the surface (Sc_s) where an ELF-value of 0.4 and 0.6 is observed in both cases. For the P_2AlAl plane, we observed a directionality of the charge that surrounds the Al atom on the surface (Al_s) and the charge surrounding the Al atom of the dimer.

Three planes P_iAlSc with $i = 1$, 2, and 3 were used for the Al-Sc dimer on the surface. For the P_1AlSc plane, results show how the charge density associated with the Al dimer atom is relocated and highly concentrated in the Sc direction. ELF values close to 0.8 were measured between the Al atom of the dimer and the Al atom of the surface (Al_1). However, in the presence of the electric field, this value decreased to between 0.4 and 0.6. For the P_2AlSc plane, we can observe small changes in charge distribution between the Al atom of the dimer and the Al atom on the surface (Al_1) generating an ELF value between 0.4 and 0.6. No significant changes were noted for the P_3AlSc plane, only a clearer charge close to the Sc atoms of the dimer and a more clear distribution over the Al atoms on the surface in the direction of the Sc atom.

These results, beyond further description of the bonding, provide a clear description of the change in the bonding character with changing electric field. In the figures, the white boxed regions show the areas of largest change with electric field. In the case of Al-Al, we identify an increased ELF value between the Al dimer atoms with increased electric field, with an ELF-value greater than 0.8 when the electric field is applied. This demonstrates that the bond is mainly covalent under electric field. Further, the bonding between the dimer and the surface atom decreases the ELF

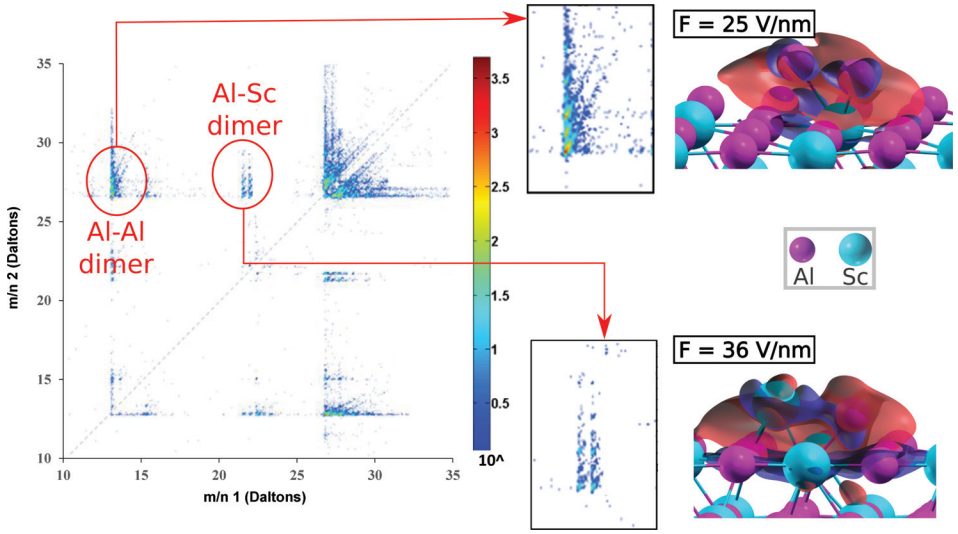

FIG. 5. (Color) Integration of APT experimental measurements with DFT data. By integrating these data we are able to include evaporation mechanisms with the data. The inset regions focus on the Al-Al dimer evaporations compared to Al-Sc dimers, with the overall chemistry of the material for these two regions being nearly equivalent. The number of Al-Al dimers is seen to be significantly higher. The DFT results indicate that charge localization (shown as dark blue) around the Sc atom results in Sc evaporating as a single ion. This figure demonstrates how DFT provides a description of evaporation mechanisms, which can then be used to interpret the experimental data.

value to less than 0.8, so that the bond between the surface and dimer loses the covalent character under electric field conditions.

For the Al-Sc case, we find decreased ELF-values between the Al atom and the surface, with the increased ELF value isolated around the Al atom. Further, the ELF-value is very low between the Sc atom and the surface. This indicates that the Sc bond does not exhibit a covalent nature under any condition, while the Al atom and the surface have weakly covalent bonding with no electric field, and no covalent bonding character when electric field is applied. These results for the Al-Sc case are in contrast to the Al-Al case, for which we identified some increase in bond strength with electric field.

Beyond providing a mechanistic model of field evaporation, this work has applications for the design of surface

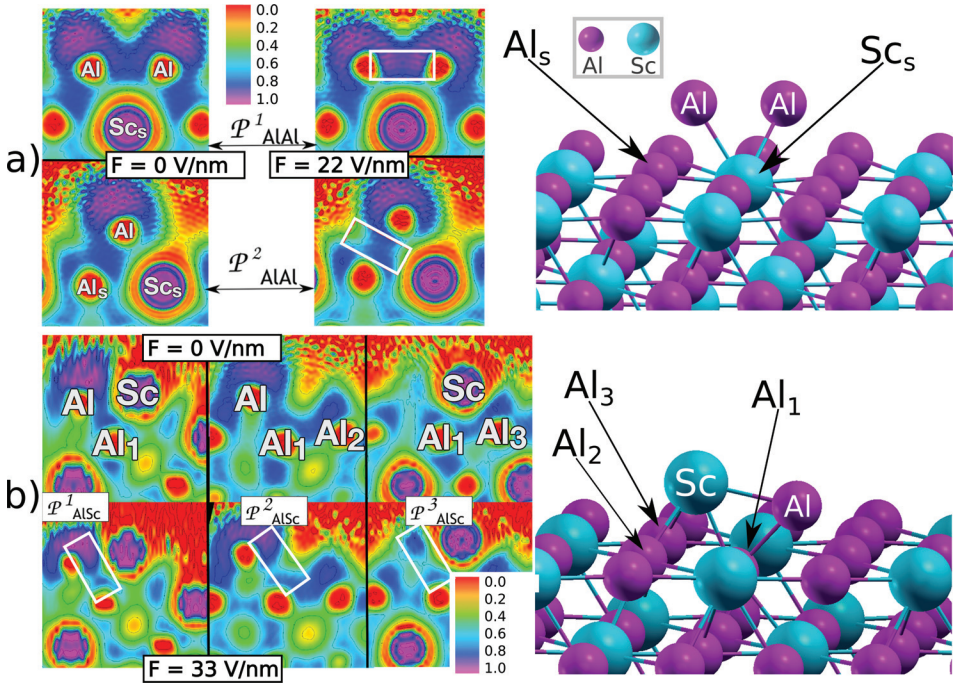

FIG. 6. (Color) Results of the ELF corresponding to the Al-Al (a) and Al-Sc (b) dimer evaporation. The plane $P^1_{Al\text{-}Al}$ shows a narrowing between the Al and Sc atoms along with a high charge density between the Al atoms of the dimer. For the plane $P^2_{Al\text{-}Al}$, a similar narrowing between the Al dimer atom and the Sc atom is observed. The boxed regions show the primary regions of change when electric field is applied, and also shows that the bonding character between the dimer ions becomes more covalent when electric field is applied.

chemistry. That is, these calculations provide a description of bonding under electric fields, so that the design of chemistry may be considered as a function of extreme electric field conditions. Further studies will increase the number of surface chemistry configurations to provide a larger library of possible surface chemistries, which will minimize the degradation of the material under extreme field conditions.

VI. CONCLUSIONS

This paper presents an approach for quantifying surface bonding under extreme conditions and provides a description of the relationship between surface chemistry and material degradation. This approach, which can also be extended to a variety of material classes and structures beyond the $L1_2$ Al-Sc structure described here, calculates the evaporation field for different surface chemistries and configurations. It was found that Al-Al surface atoms are more likely to evaporate as dimers compared with Al-Sc surface atoms, which are more likely to evaporate as single ions. Additionally, the mechanisms leading to different evaporation fields were identified. For example, Al-Al surface atoms are found to have a shared charge density, while for Al-Sc surface atoms, a charge localization occurs around the Sc atom. The integration of electric field with the APT experimental data has given insight into the relationship between bonding mechanism and electric field. This work has implications for the improved design of surface chemistries, given the degradation under extreme electric fields by linking surface chemistry with degradation mechanisms.

ACKNOWLEDGMENTS

C.L. acknowledges support from FONDECYT 11150279 and PAI 79140025 CONICYT. J.P. acknowledges support from FONDECYT 11130501, and partial support from UAB-775. S.B. and K.R. acknowledge support from the Air Force Office of Scientific Research (AFOSR) under Grant Nos. FA9550-11-1-0158 and FA9550-12-1-0456. K.R. acknowledges support from the Erich Bloch Endowed Chair at the University at Buffalo-State University of New York.

[1]B. Gault *et al.*, Ultramicroscopy **111**, 1619 (2011).
[2]E. R. McMullen and J. P. Perdew, Solid State Commun. **44**, 945 (1982).
[3]E. R. McMullen and J. P. Perdew, Phys. Rev. B **36**, 2598 (1987).
[4]S. K. Suram and K. Rajan, Microsc. Microanal. **18**, 941 (2012).
[5]J. Neugebauer and M. Scheffler, Surf. Sci. **287**, 572 (1993).
[6]C. G. Sanchez, A. Y. Lozovoi, and A. Alavi, Mol. Phys. **102**, 1045 (2004).
[7]T. Ono, T. Sasaki, J. Otsuka, and K. Hirose, Surf. Sci. **577**, 42 (2005).
[8]F. Vurpillot, S. Bostel, and D. Blavette, Ultramicroscopy **89**, 137 (2001).
[9]C. Oberdorfer and G. Schmitz, Microsc. Microanal. **17**, 15 (2011).
[10]E. A. Marquis, B. P. Geiser, T. J. Prosa, and D. J. Larson, J. Microsc. **241**, 225 (2011).
[11]B. P. Geiser, D. J. Larson, E. Oltman, S. Gerstl, D. Reinhard, T. F. Kelly, and T. J. Prosa, Microsc. Microanal. **15**, 292 (2009).
[12]T. Boll and T. Al-Kassab, Ultramicroscopy **124**, 1 (2013).
[13]P. A. Ignatiev and V. S. Stepanyuk, Phys. Rev. B **84**, 7 (2011).
[14]K. Chibane and R. G. Forbes, Surf. Sci. **122**, 191 (1982).
[15]R. G. Forbes, Ultramicroscopy **89**, 1 (2001).
[16]R. G. Forbes, Surf. Sci. **223**, 326 (1989).
[17]R. G. Forbes, J. Phys. D: Appl. Phys. **15**, 99 (1982).
[18]R. G. Forbes, C. J. Edgecombe, and U. Valdre, Ultramicroscopy **95**, 57 (2003).
[19]R. G. Forbes, Nanotechnology **23**, 095706 (2012).
[20]R. H. Fowler and L. Nordheim, Proc. R. Soc. A: Math. Phys. **119**, 173 (1928).
[21]E. L. Murphy and R. H. Good, Phys. Rev. **102**, 1464 (1956).
[22]H. J. Kreuzer, Surf. Sci. **246**, 336 (1991).
[23]H. J. Kreuzer, Surf. Interface Anal. **36**, 372 (2004).
[24]M. Karahka and H. J. Kreuzer, Ultramicroscopy **159**, 156 (2015).
[25]E. P. Silaeva, M. Karahka, and H. J. Kreuzer, Curr. Opin. Solid State Mater. **17**, 211 (2013).
[26]Y. Xia, M. Karahka, and H. J. Kreuzer, J. Appl. Phys. **118**, 025901 (2015).
[27]M. Karahka, Y. Xia, and H. J. Kreuzer, Appl. Phys. Lett. **107**, 062105 (2015).
[28]L. Yao, T. Withrow, O. D. Restrepo, W. Windl, and E. A. Marquis, Appl. Phys. Lett. **107**, 241602 (2015).
[29]J. Peralta, S. R. Broderick, and K. Rajan, Ultramicroscopy **132**, 143 (2013).
[30]P. Giannozzi *et al.*, J. Phys.: Condens. Mater. **21**, 395502 (2009).
[31]N. Marzari, D. Vanderbilt, and M. Payne, Phys. Rev. Lett. **79**, 1337 (1997).
[32]L. Bengtsston, Phys. Rev. B **59**, 12301 (1999).
[33]A. D. Becke and K. E. Edgecombe, J. Chem. Phys. **92**, 5397 (1990).
[34]K. Burdett and T. A. McCormick, J. Phys. Chem. A **102**, 6366 (1998).
[35]S. Srinivasan, K. Kaluskar, S. Broderick, and K. Rajan, Ultramicroscopy **159**, 374 (2015).
[36]S. R. Broderick, A. Bryden, S. K. Suram, and K. Rajan, Ultramicroscopy **132**, 121 (2013).
[37]S. Samudrala, O. Wodo, S. K. Suram, S. Broderick, K. Rajan, and B. Ganapathysubramanian, Comput. Mater. Sci. **77**, 335 (2013).
[38]D. W. Saxey, Ultramicroscopy **111**, 473 (2011).